Sigma J Eng Nat Sci, Vol. 44, No. 5, pp. 3143–3156, October, 2026

Sigma Journal of Engineering and Natural Sciences
Web page info: https://sigma.yildiz.edu.tr
DOI: 10.14744/sigma.2026.2148

Research Article

Simulation-based analysis of spinal joint loading in SCI patients using lower extremity exoskeletons: Anybody modeling study

İsmail ÇALIKUŞU[1,*], Uğur FİDAN[2]

[1]*Department of Electronic and Automation, Vocational School, Nevşehir Hacı Bektaş Veli University, Nevşehir, 50300, Türkiye*
[2]*Department of Biomedical Engineering, Afyon Kocatepe University, Afyonkarahisar, 03200, Türkiye*

ARTICLE INFO

Article history
Received: 02 November 2024
Revised: 13 February 2025
Accepted: 18 June 2025

Keywords:
AnyBody Modelling; Intervertebral Disc Load; Lower Extremity Exoskeleton; Spinal Cord Injury; Spinal Joint Mobility; Spinal Joints

ABSTRACT

Spinal cord injuries (SCI) often lead to serious neurological challenges—like losing mobility, impaired sensation, and reduced motor control which deeply impact a person's quality of life. In recent years, lower extremity exoskeletons (LEEs) have emerged as promising assistive technologies. These wearable devices not only help individuals walk but also relieve mechanical stress on the spine. While many studies have praised the general benefits of exoskeletons, few have taken a close look at how they influence spinal loading, especially across different phases of gait and in different user groups. This study examines people with spinal cord injury and healthy individuals walking with exoskeleton support. Spinal joint forces are calculated using the AnyBody Modeling System. Motion capture data are used in the musculoskeletal model. Spinal loads are assessed during the single and double support phases of walking. Exoskeleton use reduced overall spinal joint loading by 25–30%. Forces decreased by up to 40% in the cervical spine and about 30% in the lumbar region. In participants with spinal cord injury, the fiberglass exoskeleton reduced lumbar axial forces by up to 97%. Pelvic flexion–extension moments decreased by 91%. These results indicate lower mechanical loads during assisted walking. The use of lightweight, high-strength materials may also support spinal stability and posture, although this effect requires further evidence. Altogether, these results support the use of LEEs in rehabilitation: they don't just help people move; they actively reduce spinal stress and contribute to safer, more ergonomic mobility. Insights from this study could also help inform better design strategies for future exoskeletons, both in clinical therapy and in industrial applications.

Cite this article as: Çalıkuşu İ, Fidan U. Simulation-based analysis of spinal joint loading in SCI patients using lower extremity exoskeletons: Anybody modeling study. Sigma J Eng Nat Sci 2026;44(5):3143–3156.

INTRODUCTION

Spinal cord injury (SCI) can cause partial or complete loss of motor and sensory function below the injury level. It can also affect walking and postural control. Pain and secondary musculoskeletal complications may further limit daily activities [1, 2]. These changes provide a reason to examine spinal loading during assisted movement.

***Corresponding author.**
*E-mail address: ismailcalikusu@nevsehir.edu.tr

This paper was recommended for publication in revised form by Editor-in-Chief Ahmet Selim Dalkilic

Published by Yıldız Technical University Press, İstanbul, Turkey
© Author. This is an open access article under the CC BY-NC license (http://creativecommons.org/licenses/by-nc/4.0/).

Lower-limb exoskeletons (LEEs) provide external support to the legs and pelvis. They assist walking movements in people with impaired motor function. This support can alter ground reaction forces and the loads transmitted through the body. Exoskeletons are used in rehabilitation and have also been investigated for physically demanding workplace tasks [3–5]. Their effects depend on the device design, the activity, and the user.

Motion capture and musculoskeletal modeling allow these effects to be examined at individual joints. The AnyBody Modeling System uses movement data to estimate muscle forces and joint loads. Previous studies have reported lower spinal reaction forces, particularly in the lumbar region, under some assisted conditions [6–10]. However, comparisons between healthy individuals and people with SCI across single and double support remain limited. Published studies also differ in their use of experimental measurements, computational models, and combinations of the two [11–15].

This study examines spinal joint forces and moments during walking in healthy individuals and people with complete SCI. Joint kinematics were recorded using Kinect-based motion tracking and used as inputs to the AnyBody models. The analysis covered the cervical, thoracic, lumbar, and sacrum–pelvis regions.

Four conditions were modeled: healthy walking without an exoskeleton, healthy walking with an exoskeleton, SCI walking with an exoskeleton, and a theoretical SCI condition without assistance. The unassisted SCI condition served as a computational reference. It did not represent an observed walking trial. Single and double support were analyzed separately to examine how loading changed across gait phases.

The exoskeleton had a fiberglass frame. Previous work has considered lightweight materials and individual model parameters in exoskeleton development [16–19]. This study examined one device configuration and did not compare alternative materials. It therefore assessed loading with the modeled fiberglass exoskeleton, rather than the independent effect of fiberglass on spinal mechanics.

The study aimed to describe regional changes in spinal loading under the selected conditions. Its main elements were:

- Comparison of spinal joint forces and moments across assisted and reference walking conditions.
- Use of Kinect-derived joint kinematics as inputs to the AnyBody simulations.
- Separate analysis of single and double support.
- Examination of loading patterns across cervical, thoracic, lumbar, and sacrum–pelvis regions

MATERIALS AND METHODS

This study estimates spinal joint forces and moments during simulated walking. It includes healthy individuals and people with complete lower-limb paralysis due to spinal cord injury (SCI). Spinal loading is compared with and without exoskeleton assistance during single and double support.

Figure 1 summarizes the workflow. Motion data were collected using a Microsoft Kinect Xbox 360 sensor. Reflective markers were placed at selected anatomical landmarks. Joint trajectories were processed to obtain joint angles and identify gait phases. A three-dimensional lower-limb exoskeleton model was also developed in SolidWorks. The model included the device's mechanical structure and movement constraints. The motion data and exoskeleton model were incorporated into the AnyBody Modeling System. Four conditions were simulated: healthy walking without an exoskeleton, healthy walking with an exoskeleton, SCI walking with an exoskeleton, and a theoretical SCI condition without assistance. The last condition served as a computational reference rather than an observed walking trial.

Model settings were adjusted for each condition. In the SCI simulations, lower-limb muscles were deactivated, and upper-body compensatory mechanics were included. The exoskeleton was added to or removed from the human model according to the simulated condition. Joint reaction forces and moments were calculated from the cervical spine to the sacral region. These outputs were examined throughout the gait cycle, including transitions between single and double support. Force and moment magnitudes were compared across the four conditions. Surface plots were used to display loading patterns. These comparisons were used to assess the modeled effects of exoskeleton assistance on spinal loading [20].

The exoskeleton model (Fig. 2) was designed using SolidWorks 2016, based on a standardized human body (height: 180 cm, weight: 75 kg) to ensure physiological accuracy in the simulations. The model includes components representing the thigh, calf, foot, and hip joint of each leg. Each segment has six degrees of freedom (DOF). Joint angles were recorded using the Kinect Xbox 360 in participants with spinal cord injury (SCI) and healthy individuals. These data were used as inputs to the musculoskeletal simulation to model joint motion during exoskeleton-assisted walking.

The exoskeleton was made from A-grade fiberglass. The reported material properties were a density of approximately 1.8 g/cm^3 and a Young's modulus of about 72 GPa. Fiberglass was selected for its strength relative to its weight, corrosion resistance, and thermal stability.

Four participants from the Adana region of Türkiye took part in the study. The male participants were a 25-year-old patient with spinal cord injury (SCI) and a 23-year-old healthy participant. Both were 180 cm tall and weighed 75 kg. The female participants were a 26-year-old patient with SCI and a 21-year-old healthy participant. Both were 165 cm tall and weighed 62 kg. Height and body mass were therefore matched within each male and female pair.

Participants with SCI completed two gait cycles using a Robogait rehabilitation system at a fixed speed. Healthy

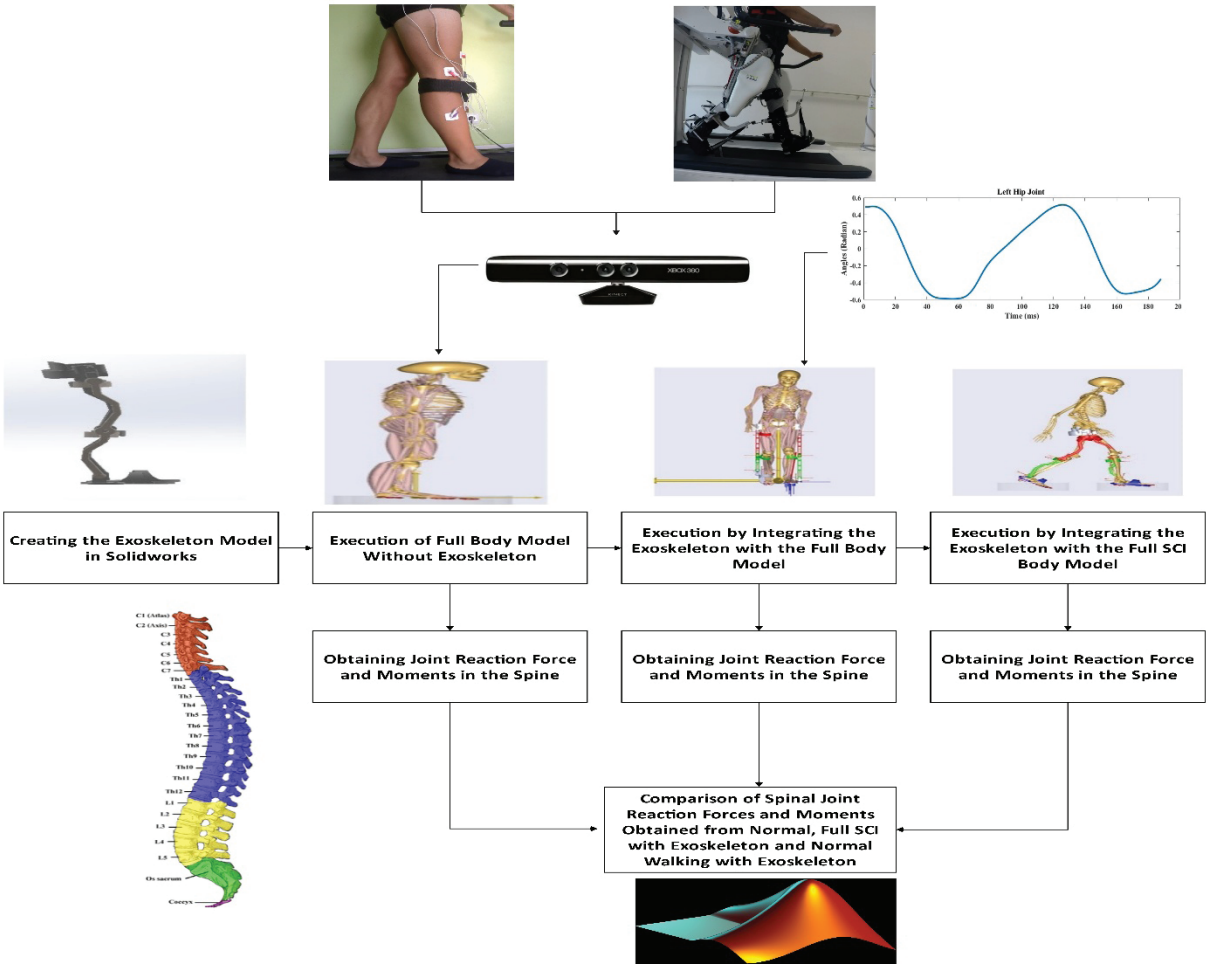


Figure 1. Biomechanical analysis of the effects of gait with and without exoskeleton on spinal joints in paralyzed and healthy individuals.

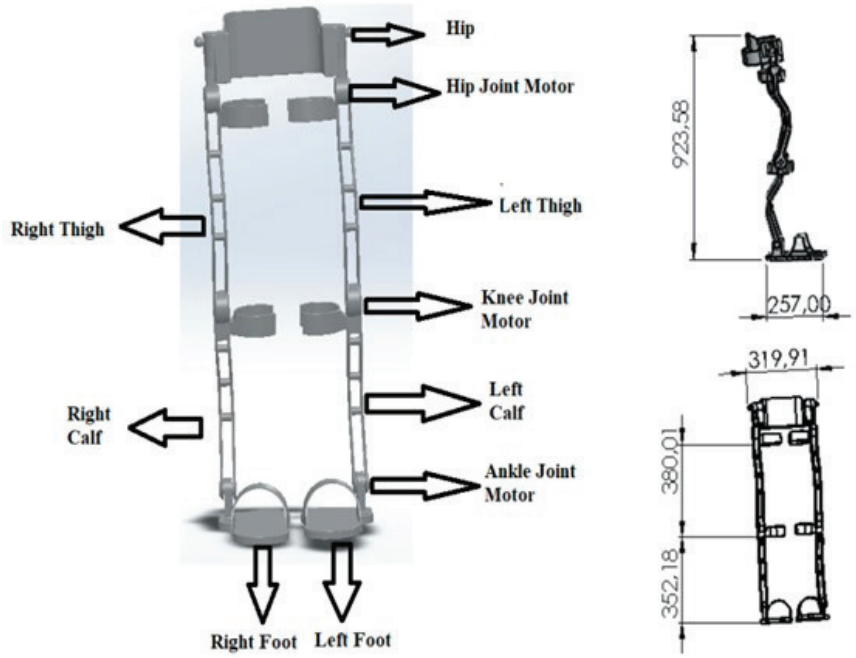


Figure 2. Fiberglass-based lower extremity exoskeleton model.

participants walked on a treadmill under the stated matching conditions. Joint movements were recorded using Kinect-based motion tracking. No missing kinematic data were reported. The recordings were then used in participant-specific AnyBody models to estimate spinal joint forces and moments. With only four participants, the study provides case-level comparisons and cannot establish effects across broader SCI or healthy populations [21].

The analysis examined two gait phases:

1. **Double support:** Both feet are in contact with the ground.
2. **Single support:** One foot is in contact with the ground.

Spinal joint loads were compared with participants with SCI and healthy participants during each gait phase. Single and double support were examined separately, with a focus on lumbar forces and moments [22].

The exoskeleton model was incorporated into the AnyBody Modelling System at the hip, thigh, calf, and foot attachment sites. The simulations estimated how these modelled attachments affected forces and moments in the musculoskeletal system.

The resulting estimates were used to compare spinal loading across the simulated walking conditions. They may inform further studies of exoskeleton design and rehabilitation use. Clinical benefits and improvements in mobility require separate evaluation.

Microsoft Xbox360 Kinect Sensor

The Microsoft Kinect for Xbox 360 tracks body movement using depth sensing and skeletal tracking. It estimates joint positions in real time, which can then be used to calculate joint angles [23].

In this study, Kinect recorded participants' movements during walking. Joint angles calculated from these recordings were entered into the musculoskeletal model. The model used these inputs to estimate spinal joint forces and moments during exoskeleton-assisted walking.

AnyBody Modelling System

The AnyBody Modelling System is a musculoskeletal simulation platform developed from research at Aalborg University [24]. It is used to estimate muscle forces and joint loads during human movement. The model used in this study comprised 25 anatomical segments, 16 joints, and 804 muscles [25, 26]. These counts describe the selected model configuration.

The platform allows model parameters to be adjusted to participant characteristics. It also accepts motion data from external tools as simulation inputs. In this study, the single and double support phases of gait were analyzed separatelySpinal joint forces and moments were estimated for each gait phase. The estimates were then compared across walking conditions to examine changes in spinal loading with exoskeleton assistance.

Phases of Double Support and Single Support in the Gait Cycle

The model estimates joint and muscle loads using each participant's anatomical characteristics. In this study, the double and single support phases of gait were analyzed separately using the AnyBody Modeling System. Figure 3

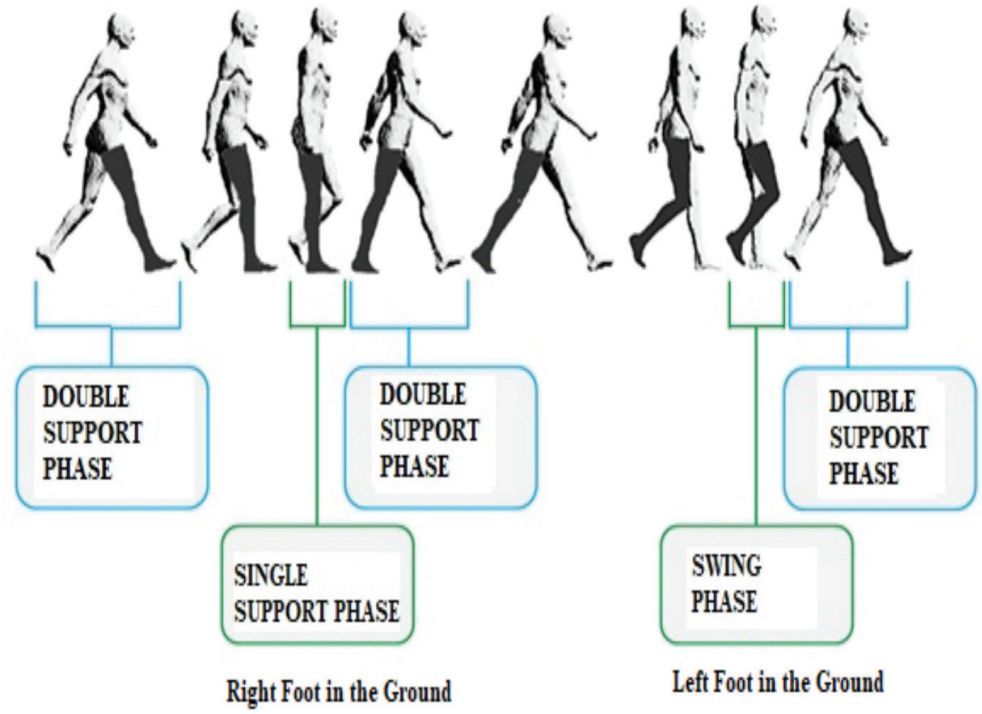


Figure 3. Double support and single support in human gait.

illustrates these phases and their transitions according to foot contact with the ground. Spinal joint loads were examined during each phase to assess the modeled effects of exoskeleton-assisted walking [27].

This study employed an AnyBody model to simulate gait cycles, including 4 double support phases and 3 single support phases (time duration is given in Table 1).

RESULTS AND DISCUSSION

In this study, the average spinal joint reaction forces and moments during seven distinct gait phases were obtained for three cases: a healthy person's gait without an exoskeleton, a healthy person's gait with an exoskeleton, and an SCI patient's gait with a LEE exoskeleton made from Type A fiberglass.

Spinal Joint Reaction Forces During Unskeletonized Gait in Healthy Individuals

Human gait is a complex biomechanical process that generates varying levels of force along the spinal column. As shown in Table 2, spinal joint loading fluctuates considerably throughout different phases of the gait cycle. Among all spinal regions, the cervical joints—responsible for supporting head and neck movements—experience the highest forces. This is primarily due to the abrupt transfer of body weight during heel strike (Phase 1) and the dynamic shifting of weight during phases 3, 5, and 7. The T1–C7 joint, located at the junction of the cervical and thoracic spine, showed relatively low reaction forces during the analyzed gait phases. Its loading pattern differed from those of the lumbar and sacrum–pelvis regions. Structural support from the thoracic region may help explain this difference, although the simulations did not directly test this explanation.

Table 2 presents spinal joint reaction forces in a healthy participant across seven phases of two gait cycles. It includes forces in the cervical, thoracic, lumbar, and sacrum–pelvis regions.

Reaction forces were higher in the lumbar region than in the cervical and upper thoracic regions. The sacrum–pelvis joint showed the highest forces across all analyzed phases. This pattern is consistent with the transfer of upper-body loads through the lower spine to the pelvis. However, the estimated forces also depend on the model configuration and the recorded movement patterns.

The results indicate that loading was distributed unevenly along the spine during walking. Examining each region separately allows changes in cervical, thoracic, lumbar, and sacrum–pelvis loading to be compared. This approach can help identify where exoskeleton assistance changes joint forces within the modeled walking conditions.

of region-specific analysis when evaluating the biomechanical effects of assistive devices such as exoskeletons.

Spinal Joint Reaction Forces During Gait in a Healthy Person with a Fiberglass Exoskeleton

The change in reaction forces occurring in the spine of a healthy person while Gait with LEE made of A Glass Fiber material is shown in Table 3.

Table 3 compares spinal joint reaction forces during walking with and without exoskeleton assistance. The largest forces occurred in the proximodistal direction across all spinal regions. Double support phases were more frequent than single support phases during assisted walking. This observation alone does not establish greater gait stability.

Joint reaction forces were lower with exoskeleton assistance at all analysed joints. In the cervical region, assistance reduced the increase in loading from C1 to C6. Forces decreased by 14–53% in the anteroposterior direction, 30–68% in the mediolateral direction, and 30–45% in the proximodistal direction.

In the lumbar region, reductions ranged from 32–90% anteroposteriorly, 40–58% mediolaterally, and 31–33% proximodistally. Forces also decreased at the lower lumbar and sacrum–pelvis joints, including L5–sacrum, across all reported directions. At T12–L1 and C7–T1, reductions ranged from approximately 19–54%, depending on the force component.

These results indicate lower estimated spinal forces during exoskeleton-assisted walking under the modelled conditions. The size of the reduction varied by joint and direction. The simulations did not assess musculoskeletal strain or chronic back and neck pain. Longer-term clinical studies would be needed to evaluate those outcomes.

Table 1. Single support and double support phases and their duration intervals

Phase No	Time Interval (mS)	Left	Right	Phase Type
Phase 1	1.62-1.72	Stance	Stance	Double Support
Phase 2	1.73-2.17	Swing	Stance	Single Support
Phase 3	2.18-2.30	Stance	Stance	Double Support
Phase 4	2.31-2.76	Stance	Swing	Single Support
Phase 5	2.77-2.91	Stance	Stance	Double Support
Phase 6	2.92-3.35	Swing	Stance	Single Support
Phase 7	3.36-3.47	Stance	Stance	Double Support

Table 2. Spinal Joint Reaction Forces During Healthy Human Gait

Joint Reaction Forces		Walking with a Fiberglass-Based Exoskeleton						
		Faz 1	**Faz 2**	**Faz 3**	**Faz 4**	**Faz 5**	**Faz 6**	**Faz 7**
C1 C0	Anterior Posterior Force	-15.29	-12.51	-12.51	-12.51	-13.51	-26.51	-22.60
	MedioLateral Force	-32.05	-7.87	-1.01	-1.79	-14.19	-10.27	-1.67
	Proksimo Distal Force	121.40	102.49	136.29	100.42	120.03	91.57	150.79
C2 C1	Antero Posterial Force	-13.57	-11.36	-13.72	-18.68	-23.06	-26.61	-39.74
	Medio Lateral Force	-35.92	-6.66	-7.17	-9.32	-20.83	-10.68	-12.64
	Proksimo Distal Force	-13.57	-11.36	-13.72	-18.68	-23.06	-26.61	-39.74
C3 C2	AnteroPosteriorForce	-16.90	-14.62	-17.87	-20.43	-24.46	-27.51	-39.62
	MedioLateralForce	-36.35	-3.95	-7.38	-11.93	-22.70	-9.58	-15.82
	ProksimoDistalForce	155.44	128.16	167.88	128.44	153.23	122.81	203.64
C4 C3	Antero Posterial Force	-19.88	-16.87	-21.58	-20.53	-23.74	-26.91	-37.04
	Medio Lateral Force	-34.34	-0.52	-6.66	-14.88	-23.68	-8.20	-20.09
	Proksimo Distal Force	173.27	142.73	187.18	147.36	174.97	139.82	234.96
C5 C4	Antero Posterial Force	-16.90	-14.62	-17.87	-20.43	-24.46	-27.51	-39.62
	Medio Lateral Force	-30.86	2.63	-9.50	-18.24	-24.50	-6.33	-24.62
	Proksimo Distal Force	194.02	159.22	210.01	165.26	196.28	158.08	265.64
C6 C5	Antero Posterial Force	-26.38	-24.89	-31.40	-24.97	-25.47	-26.99	-35.87
	Medio Lateral Force	-27.26	3.62	-10.63	-18.44	-22.27	-3.99	-24.85
	Proksimo Distal Force	207.00	169.68	224.63	176.12	209.20	168.37	284.08
C7 C6	Antero Posterial Force	-32.12	-31.34	-39.02	-28.83	-28.64	-29.10	-37.98
	Medio Lateral Force	-24.32	3.56	-9.58	-16.23	-19.75	-4.05	-21.01
	Proksimo Distal Force	209.31	170.83	226.26	177.81	211.87	170.19	286.84
L1 L2	Antero Posterial Force	-288.51	-262.41	-315.02	-243.05	-274.28	-261.14	-385.94
	Medio Lateral Force	-62.85	-19.93	54.23	27.46	-28.06	-29.53	75.74
	Proksimo Distal Force	1272.36	1075.23	1326.42	999.06	1153.79	1047.64	1596.82
L2 L3	Antero Posterial Force	-153.15	-138.96	-179.03	-136.16	-139.45	-142.15	-212.23
	Medio Lateral Force	-31.86	-8.80	29.59	9.12	-16.94	-16.37	38.00
	Proksimo Distal Force	1253.30	1050.37	1313.69	990.61	1122.07	1025.39	1574.36
L3 L4	Antero Posterial Force	14.58	0.49	3.94	6.70	10.08	5.96	8.29
	Medio Lateral Force	18.38	14.95	-11.21	-19.65	-2.81	11.06	-14.32
	Proksimo Distal Force	1194.25	1013.43	1251.16	960.76	1089.24	986.22	1490.76
L4 L5	Antero Posterial Force	169.98	143.81	176.46	138.90	158.51	148.80	215.64
	Medio Lateral Force	40.81	18.92	-29.86	-24.30	10.39	19.51	-41.35
	Proksimo Distal Force	1193.41	1018.56	1240.85	961.79	1098.14	983.68	1490.95
L5 Sacrum	Antero Posterial Force	180.10	168.87	188.68	158.79	184.70	174.19	245.65
	Medio Lateral Force	50.26	23.85	-37.05	-31.26	11.79	26.21	-50.28
	Proksimo Distal Force	1285.29	1086.96	1343.38	1028.46	1183.98	1046.65	1596.21
Sacrum Pelvis	Antero Posterial Force	202.58	182.84	206.98	172.19	200.03	189.81	270.31
	Medio Lateral Force	55.40	24.79	-41.42	-33.06	13.94	27.25	-56.63
	Proksimo Distal Force	1412.90	1145.52	1429.33	1085.91	1085.91	1112.83	1704.65
T12 L1	Antero Posterial Force	187.95	-343.09	-412.30	-319.70	-370.86	-346.20	-503.35
	Medio Lateral Force	-83.03	-41.25	75.92	61.56	-21.13	-45.08	119.00
	Proksimo Distal Force	1268.67	1046.20	1298.01	982.38	1133.49	1015.29	1537.76
T1 C7	Antero Posterial Force	-37.55	-37.72	-46.17	-31.60	-31.14	-31.04	-38.56
	Medio Lateral Force	-18.66	2.81	-7.53	-9.18	-12.39	-4.27	-14.21
	Proksimo Distal Force	216.25	172.81	231.31	190.22	223.42	172.92	299.68

Table 3. Changes in spinal reaction forces during gait in a healthy person with a fiberglass exoskeleton

Spine Joint Reaction Forces		Walking without Exoskeleton						
		Phase 1 (N)	Phase 2 (N)	Phase 3 (N)	Phase 4 (N)	Phase 5 (N)	Phase 6 (N)	Phase 7 (N)
C1 C0	Anetrior Posterior Force	-14.60	-5.65	-13.16	-13.16	-13.16	-17.33	-18.67
	Medio Lateral Force	-14.86	-5.45	2.50	0.15	-9.36	-3.43	-0.26
	Proksimo Distal Force	86.83	68.19	91.04	66.94	89.81	65.93	89.62
C2 C1	Antero Posterial Force	-13.99	-5.01	-13.62	-10.69	-18.91	-17.71	-25.92
	Medio Lateral Force	-16.70	-5.70	-0.78	-1.70	-11.56	-4.38	-4.79
	Proksimo Distal Force	-13.99	-5.01	-13.62	-10.69	-18.91	-17.71	-25.92
C3 C2	Antero Posterial Force	-16.65	-7.44	-16.86	-12.28	-21.14	-18.38	-26.49
	Medio Lateral Force	-15.42	-5.15	-2.92	-2.23	-2.23	-4.01	-6.98
	Proksimo Distal Force	112.93	86.14	117.86	86.36	117.13	88.44	121.96
C4 C3	Antero Posterial Force	-19.41	-10.10	-20.13	-13.65	-21.61	-18.39	-26.55
	Medio Lateral Force	-13.72	-4.70	-5.50	-2.84	-10.84	-3.49	-9.11
	Proksimo Distal Force	100.50	77.54	104.89	76.98	104.04	77.37	106.04
C5 C4	Antero Posterial Force	-16.65	-7.44	-16.86	-12.28	-21.14	-18.38	-26.49
	Medio Lateral Force	-11.71	-4.52	-8.50	-3.45	-10.24	-2.89	-11.37
	Proksimo Distal Force	138.06	104.27	144.28	105.50	144.06	111.67	152.98
C6 C5	Antero Posterial Force	-26.03	-16.57	-29.13	-17.65	-24.79	-19.64	-28.04
	Medio Lateral Force	-8.79	-4.25	-10.65	-3.10	-8.51	-1.89	-12.48
	Proksimo Distal Force	147.66	111.34	154.06	112.70	154.20	119.42	164.11
C7 C6	Antero Posterial Force	-30.55	-20.79	-34.79	-20.23	-27.43	-21.23	-29.61
	Medio Lateral Force	-6.48	-4.19	-9.99	-1.79	-6.88	-1.76	-10.37
	Proksimo Distal Force	149.66	112.78	155.76	114.39	156.72	121.29	166.74
L1 L2	Antero Posterial Force	-212.53	-152.79	-230.75	-150.63	-220.50	-177.65	-215.75
	Medio Lateral Force	-30.74	-5.34	28.91	2.57	-29.23	-6.91	19.25
	Proksimo Distal Force	890.09	644.90	939.92	628.13	949.84	727.15	928.80
L2 L3	Antero Posterial Force	-118.01	-77.63	-133.07	-78.05	-111.98	-93.30	-106.39
	Medio Lateral Force	-16.90	-0.55	17.05	-4.01	-20.54	-1.84	5.88
	Proksimo Distal Force	863.75	630.18	916.49	615.84	920.89	707.97	905.19
L3 L4	Antero Posterial Force	1.31	9.30	1.41	9.16	19.76	17.04	20.08
	Medio Lateral Force	7.63	6.84	-5.02	-12.70	-1.57	5.47	-16.61
	Proksimo Distal Force	852.68	621.54	909.71	608.53	902.37	698.90	881.32
L4 L5	Antero Posterial Force	-14.60	-5.65	-13.16	-10.24	-18.67	-17.33	-25.23
	Medio Lateral Force	16.66	7.30	-13.75	-10.09	8.04	6.04	-17.19
	Proksimo Distal Force	847.77	622.91	906.73	613.05	896.85	694.92	877.05
L5 Sacrum	Antero Posterial Force	148.05	107.96	159.79	108.96	165.26	133.24	159.23
	Medio Lateral Force	22.62	9.40	-18.24	-15.70	11.26	11.56	-21.26
	Proksimo Distal Force	923.28	680.42	985.69	663.29	960.37	742.88	942.66
Sacrum Pelvis	Antero Posterial Force	179.37	119.76	193.30	119.93	192.88	147.74	186.70
	Medio Lateral Force	-103.42	-12.49	106.89	4.64	-90.15	-12.09	66.59
	Proksimo Distal Force	1110.86	720.56	1167.65	696.28	1105.59	793.63	1076.36
T12 L1	Antero Posterial Force	-287.15	-208.16	-308.41	-202.86	-304.17	-243.84	-294.56
	Medio Lateral Force	-37.97	-12.90	38.62	18.69	-22.23	-13.38	36.57
	Proksimo Distal Force	872.50	636.39	918.58	616.39	936.13	719.97	904.24
T1 C7	Antero Posterial Force	-34.76	-24.91	-40.19	-22.52	-29.71	-22.51	-30.85
	Medio Lateral Force	-2.04	-4.32	-9.42	0.97	-2.94	-1.86	-7.80
	Proksimo Distal Force	155.47	115.60	159.54	119.04	163.40	125.66	171.11

Changes in Spinal Joint Reaction Forces During Gait in a Full SCI Patient with a Fiberglass Exoskeleton

Spinal cord injury (SCI) can affect movement and sensation below the injury level. Some people retain the ability to walk, while others require assistance. Lower-limb exoskeletons support the legs and pelvis during walking.

This study used simulations to examine spinal loading with a fiberglass exoskeleton. Table 4 shows the estimated

Table 4. Spinal joint reaction forces of a completed SCI patient gait with a fiberglass LEE

Joint Reaction Forces		Completed SCI Patient Walking with a Glass Fiber Exoskeleton						
		Phase 1 (N)	Phase 2 (N)	Phase 3 (N)	Phase 4 (N)	Phase 5 (N)	Phase 6 (N)	Phase 7 (N)
C1	Anterior Posterior Force	-5.47	-7.99	-3.55	-9.12	-12.58	-19.81	-19.67
C0	Medio Lateral Force	-34.01	-11.81	-11.81	9.30	-6.40	-12.43	13.02
	Proksimo Distal Force	80.75	63.65	77.66	58.54	76.70	59.79	74.82
C2	Antero Posterial Force	-2.51	-6.59	-3.69	-9.41	-12.39	-19.13	-19.98
C1	Medio Lateral Force	-13.57	-11.36	-13.72	-18.68	-23.06	-26.61	-39.74
	Proksimo Distal Force	-2.51	-6.59	-3.69	-9.41	-12.39	-19.13	-19.98
C3	Antero Posterial Force	-3.71	-8.47	-5.79	-10.37	-13.18	-19.53	-19.80
C2	Medio Lateral Force	-36.39	-13.48	9.39	8.00	-9.26	-13.51	10.99
	Proksimo Distal Force	103.04	80.41	98.05	75.33	98.69	79.93	99.34
C4	Antero Posterial Force	-5.08	-10.61	-8.05	-11.37	-13.64	-19.80	-19.39
C3	Medio Lateral Force	-36.66	-14.11	-14.11	8.40	-9.13	-13.77	11.50
	Proksimo Distal Force	91.67	72.23	87.90	67.08	87.71	70.02	87.01
C5	Antero Posterial Force	-3.71	-8.47	-5.79	-10.37	-13.18	-19.53	-19.80
C4	Medio Lateral Force	-36.73	-14.93	9.24	9.06	-8.67	-14.28	12.37
	Proksimo Distal Force	125.99	96.19	119.08	91.27	121.21	98.54	122.81
C6	Antero Posterial Force	-10.56	-17.02	-15.01	-14.78	-15.98	-21.72	-20.29
C5	Medio Lateral Force	-37.84	-16.25	10.22	10.94	-7.68	-15.39	15.45
	Proksimo Distal Force	134.67	101.92	127.10	96.94	129.30	104.86	130.22
C7	Antero Posterial Force	-14.21	-20.92	-19.64	-17.15	-18.17	-23.25	-21.76
C6	Medio Lateral Force	-36.36	-16.48	11.09	12.39	-6.18	-15.69	17.57
	Proksimo Distal Force	137.61	103.39	129.06	98.55	131.80	106.74	132.29
L1	Antero Posterial Force	-13.87	2.07	0.64	2.25	-3.95	3.31	-21.53
L2	Medio Lateral Force	1.30	-3.88	-1.47	3.88	4.58	-4.27	-1.06
	Proksimo Distal Force	35.03	-20.06	-7.67	-18.23	-2.29	-28.08	85.75
L2	Antero Posterial Force	-8.57	0.24	0.44	0.33	-2.53	-0.11	-13.05
L3	Medio Lateral Force	-0.39	-3.37	-0.15	3.73	3.22	-3.66	-0.86
	Proksimo Distal Force	62.85	5.15	21.72	6.39	6.39	-1.51	-1.51
L3	Antero Posterial Force	1.23	3.60	4.64	3.58	5.15	2.57	1.37
L4	Medio Lateral Force	0.47	-2.66	0.03	3.18	2.24	-2.83	-0.15
	Proksimo Distal Force	89.20	27.27	47.91	28.52	57.10	22.05	22.05
L4	Antero Posterial Force	-5.47	-7.99	-3.55	-9.12	-12.58	-19.81	-19.67
L5	Medio Lateral Force	0.89	-0.73	-0.43	0.91	0.92	-0.81	-1.63
	Proksimo Distal Force	113.33	46.30	71.67	47.26	81.95	41.88	159.57
L5	Antero Posterial Force	31.64	18.18	25.14	18.76	28.35	17.31	38.21
Sacrum	Medio Lateral Force	0.87	1.21	-0.55	-1.39	-0.60	1.09	-2.53
	Proksimo Distal Force	141.24	62.76	96.06	63.55	105.45	58.04	188.26
Sacrum	Antero Posterial Force	32.53	18.60	25.75	19.19	29.08	17.78	39.66
Pelvis	Medio Lateral Force	1.00	1.28	-0.65	-1.52	-0.62	1.13	-2.97
	Proksimo Distal Force	141.04	62.63	95.90	63.42	105.25	57.90	187.95
T12	Antero Posterial Force	-13.71	6.43	3.60	5.26	0.34	10.63	-25.02
L1	Medio Lateral Force	5.52	-2.95	-4.59	1.37	6.25	-3.63	-2.60
	Proksimo Distal Force	-0.99	-48.17	-42.42	-42.42	-41.32	-55.83	47.97
T1	Antero Posterial Force	-17.98	-24.62	-24.39	-19.30	-20.31	-24.38	-22.96
C7	Medio Lateral Force	-34.62	-17.04	11.86	15.27	-4.52	-16.49	20.14
	Proksimo Distal Force	140.35	106.95	130.64	102.85	134.82	111.54	135.85

joint forces, which were lower with assistance in all spinal regions examined.

Lower-limb muscles were deactivated in the SCI models. The reductions therefore describe changes under this assumption. External support altered how loads were transferred through the model, but the simulations did not assess long-term spinal health or tissue damage.

Building upon the earlier analyses, this section compares spinal joint reaction forces during exoskeleton-assisted walking to those observed in healthy individuals walking without an exoskeleton (Table 2). The comparative evaluation reveals that the exoskeleton significantly reduces joint reaction forces across all analyzed spinal segments, with the most pronounced decrease observed in the lumbar and pelvic regions.

In the cervical spine, the exoskeleton effectively mitigated the natural progressive increase in loading from vertebrae C1 to C6. Specifically, joint reaction forces were reduced by 34–53% in the anteroposterior direction, 79–95% in the mediolateral direction, and 39–52% in the proximodistal (vertical) direction. The reductions indicate lower loading in the upper spinal segments during the simulated walking conditions. Larger reductions were observed in the lumbar region. Lumbar forces decreased by 46–97% in the anteroposterior direction, 40–58% in the mediolateral direction, and 93–97% in the proximodistal direction.

At the L5–sacrum and sacrum–pelvis joints, reaction forces decreased by approximately 87–96% across all three directions. Reductions at T12–L1 approached 97% in each direction. At C7–T1, forces decreased by 38% in the anteroposterior direction and by more than 88% in the mediolateral and proximodistal directions.

These findings indicate that exoskeleton assistance reduced estimated spinal joint forces within the modelled conditions. The largest reductions occurred in the lower back and pelvic regions. This pattern may be relevant to spinal load management during assisted walking in people with SCI. However, reduced joint forces alone do not demonstrate pain relief or improved rehabilitation outcomes. Potential benefits for chronic neck or lower back pain require clinical evaluation.

Joint Reaction Moments Occurring in Single and Double Support Phases as a Result of Gait of a Healthy Person

Table 5 presents spinal joint reaction moments across seven gait phases (Phases 1–7) in a healthy participant. Moments at the cervical joints (C1–C7) remained positive throughout these phases. The positive values indicate a

Table 5. Spinal joint reaction moments obtained from a healthy human walking

Spine Joint Reaction Moment		Spinal Joint Reaction Moments of a Normal Person During Walking						
		Phase 1 (Nm)	Phase 2 (Nm)	Phase 3 (Nm)	Phase 4 (Nm)	Phase 5 (Nm)	Phase 6 (Nm)	Phase 7 (Nm)
C1 C0	Extension Moment	-0.95	-0.62	-0.94	-0.69	-1.05	-0.78	-1.01
C2 C1	Axial Moment	-0.27	-0.12	-0.28	-0.18	-0.23	-0.07	-0.22
C3 C2	Axial Moment	-0.19	-0.07	-0.35	-0.21	-0.20	-0.02	-0.30
	Extension Moment	-1.61	-1.32	-1.65	-1.18	-1.52	-0.98	-1.20
	Lateral Moment	-0.10	0.32	0.75	0.21	-0.08	0.14	0.46
C4 C3	Axial Moment	-0.16	-0.04	-0.42	-0.24	-0.18	0.01	-0.40
	Extension Moment	-1.67	-1.41	-1.72	-1.24	-1.55	-0.98	-1.19
	Lateral Moment	-0.31	0.27	0.67	0.15	-0.27	0.10	0.29
C5 C4	Axial Moment	-0.12	-0.04	-0.50	-0.26	-0.17	0.04	-0.50
	Extension Moment	-1.61	-1.44	-1.65	-1.19	-1.45	-0.89	-1.04
	Lateral Moment	-0.56	0.21	0.52	0.05	-0.50	0.04	0.04
C6 C5	Axial Moment	-0.06	-0.01	-0.61	-0.29	-0.13	0.08	-0.62
	Extension Moment	-1.22	-1.19	-1.23	-0.90	-1.04	-0.55	-0.58
	Lateral Moment	-0.73	0.16	0.37	-0.01	-0.66	0.02	-0.19
C7 C6	Axial Moment	-0.02	0.02	-0.53	-0.27	-0.09	0.09	0.09
	Extension Moment	0.23	-0.15	0.32	0.17	0.44	0.60	1.02
	Lateral Moment	-0.88	0.09	0.21	-0.06	-0.80	-0.02	-0.39
Sacrum Pelvis	Axial Moment	-7.60	-1.37	7.38	1.37	-5.90	-1.50	5.36
	Flexion Extension Moment	-1.49	5.02	-0.37	5.20	1.28	1.89	1.89
	Lateral Moment	1.54	0.17	-1.16	-0.23	0.93	0.24	-0.91
T1 C7	Axial Moment	0.05	0.04	-0.46	-0.21	0.02	0.09	-0.48
	Extension Moment	1.81	1.07	2.10	1.32	2.01	1.86	2.80
	Lateral Moment	-0.97	0.00	0.04	-0.06	-0.89	-0.07	-0.58

consistent moment direction under the model's coordinate convention. They do not, by themselves, establish muscle activity or the purpose of the moments.

The cervical moment patterns describe the modeled mechanical loading during unassisted walking. Their relationship to head posture and upper-body balance requires consideration of the joint axes and recorded movements. These results provide a reference for comparisons with exoskeleton-assisted walking and the SCI simulations.

A detailed analysis of Table 5 reveals that joint reaction moments in the spine vary significantly between the double and single support phases of the gait cycle. In general, higher moment values are observed during double support phases, reflecting the increased mechanical demands of weight transfer and stabilization during these periods. However, region-specific variations in moment patterns provide further insight into the dynamic behavior of spinal segments during locomotion.

In the cervical spine (C1–C7), axial moments tend to decrease during double support and increase during single support, whereas extension and lateral bending moments exhibit the opposite trend—rising in double support and decreasing in single support. This suggests that the cervical spine actively compensates for balance and head stabilization, particularly during gait phases when one foot is off the ground. Joint moments generally increased across Phases 1–7. This trend describes changes in spinal loading over the analyzed gait cycle, but does not alone establish an increase in stabilization demands.

At the sacrum–pelvis joint, moment patterns differed between support phases. Axial moments decreased during double support and increased during single support. Flexion moments decreased consistently during double support but followed a nonlinear pattern during single support. Lateral bending moments showed the opposite trend: they increased during double support and decreased during single support. Pelvic motion and movement of the opposite limb may contribute to these patterns, although their contributions were not directly tested.

At C7–T1, positive moments increased during double support, while negative moments decreased. During single support, increases were reported in both positive and negative moments. Extension moments also increased progressively during both support phases. These changes describe phase-dependent loading at the cervical–thoracic junction. Further analysis would be needed to relate them to trunk control or upper-body balance.

Table 6. Spinal joint reaction moments of a healthy person during gait with LEE

Spine Joint Reaction Moments		Spinal Joint Reaction Moments of a Normal Person During Walking with LEE						
		Phase 1 (Nm)	Phase 2 (Nm)	Phase 3 (Nm)	Phase 4 (Nm)	Phase 5 (Nm)	Phase 6 (Nm)	Phase 7 (Nm)
C1 C0	Extension Moment	-1.31	-1.06	-1.53	-1.23	-1.49	-1.32	-2.27
C2 C1	Axial Moment	-0.42	-0.02	-0.64	-0.77	-0.70	-0.03	-0.75
C3 C2	Axial Moment	-0.33	0.15	-0.71	-0.86	-0.71	0.09	-0.82
	Extension Moment	-2.45	-1.93	-2.65	-1.81	-2.12	-1.54	-2.78
	Lateral Moment	-0.01	0.24	1.39	0.61	0.09	0.10	0.95
C4 C3	Axial Moment	-0.28	0.28	-0.70	-0.91	-0.67	0.17	-0.90
	Extension Moment	-2.69	-2.08	-2.92	-1.99	-2.31	-1.56	-2.99
	Lateral Moment	-0.50	0.26	1.37	0.31	-0.37	-0.01	0.50
C5 C4	Axial Moment	-0.26	0.36	-0.70	-0.95	-0.63	0.25	-0.98
	Extension Moment	-2.82	-2.16	-3.09	-2.04	-2.36	-1.47	-3.04
	Lateral Moment	-1.02	0.37	1.17	-0.14	-0.94	-0.11	-0.12
C6 C5	Axial Moment	-0.14	0.42	-0.75	-1.01	-0.57	0.38	-1.08
	Extension Moment	-2.43	-1.82	-2.69	-1.66	-1.92	-1.00	-2.48
	Lateral Moment	-1.50	0.44	1.03	-0.44	-1.32	-0.16	-0.55
C7 C6	Axial Moment	0.02	0.41	-0.64	-0.89	-0.43	0.40	-0.91
	Extension Moment	-0.57	-0.23	-0.62	-0.03	-0.06	0.61	0.07
	Lateral Moment	-1.94	0.48	0.89	-0.71	-1.67	-0.24	-0.94
Sacrum Pelvis	Axial Moment	-0.53	-0.40	0.39	0.52	-0.04	-0.41	0.58
	Flexion Extension Moment	6.52	8.19	9.76	7.65	8.93	6.97	10.64
	Sacrum Pelvis Lateral Moment	0.95	0.60	-0.72	-0.77	0.15	0.64	-1.00
T1 C7	Axial Moment	0.22	0.37	-0.52	-0.62	-0.14	0.41	-0.68
	Extension Moment	1.48	1.67	1.75	1.47	1.78	2.46	2.63
	Lateral Moment	-2.35	0.50	0.75	-0.89	-1.94	-0.34	-1.25

Joint Reaction Moments Occurring in Single and Double Support Phases as a Result of a Healthy Person Gait with LEE

Table 6 shows the joint reaction moments in the spine as a result of a healthy individual gait with LEE in the seven phases of the gait cycle (Phases 1-7).

Exoskeletons have demonstrated considerable potential in assisting individuals with mobility impairments by partially restoring or enhancing walking ability. However, their biomechanical impact on different spinal regions is not uniformly positive and requires nuanced evaluation. In the cervical spine, for instance, the effects of exoskeleton use are complex and somewhat contradictory. The extension moment decreased by approximately 47%, and overall load decreased by 31%. However, the lateral bending moment increased by 85%, particularly at C6–C7. This indicates that exoskeleton assistance reduced some loading components while increasing others. The simulations did not establish whether the increase causes discomfort or tissue strain. Its relationship to exoskeleton mass and weight distribution also requires further investigation.

At the sacrum–pelvis joint, axial load decreased by approximately 83%. The extension moment increased by 22%, while the lateral bending moment decreased by 72%. These changes show a different loading pattern from that observed in the cervical region. They do not, on their own, demonstrate improved stability or protection against injury.

At C7–T1, both axial and lateral moments increased. The extension moment also increased by up to 30%. These results suggest that exoskeleton assistance altered loading at the cervical–thoracic junction. The simulations did not determine whether these changes resulted from compensatory movement, device alignment, or support elsewhere along the spine.

The effects of exoskeleton assistance therefore varied by spinal region and loading component. Reductions in one region occurred alongside increases in another. These patterns should be considered when evaluating the device configuration. Further analyses could examine how attachment position, alignment, and mass distribution affect spinal forces and moments.

Joint Reaction Moments Occurring in Single and Double Support Phases as a Result of a Person with SCI Gait with LEE

Table 7 shows the joint reaction moments in the spine because of LEE Gait by an individual with completed spinal

Table 7. Spinal joint reaction moments of a person with completed SCI during gait with LEE

Spine Joint Reaction Moments		Spinal Joint Reaction Moments of a Person with Completed SCI During Walking with LEE						
		Phase 1 (Nm)	Phase 2 (Nm)	Phase 3 (Nm)	Phase 4 (Nm)	Phase 5 (Nm)	Phase 6 (Nm)	Phase 7 (Nm)
C1 C0	Extension Moment	-0.64	-0.50	-0.58	-0.46	-0.70	-0.59	-0.58
C2 C1	Axial Moment	-0.22	-0.14	-0.17	-0.13	-0.16	-0.03	-0.12
C3 C2	Axial Moment	-0.13	-0.10	-0.21	-0.18	-0.18	0.03	-0.16
	Extension Moment	-1.50	-0.96	-1.48	-0.82	-1.15	-0.49	-0.66
	Lateral Moment	0.18	0.21	0.23	0.03	0.05	0.10	0.13
C4 C3	Axial Moment	-0.17	-0.12	-0.21	-0.19	-0.21	0.03	-0.15
	Extension Moment	-1.67	-1.00	-1.62	-0.84	-1.19	-0.41	-0.61
	Lateral Moment	-0.29	0.04	0.35	0.12	-0.07	-0.08	0.22
C5 C4	Axial Moment	-0.24	-0.15	-0.19	-0.17	-0.24	0.01	-0.13
	Extension Moment	-1.79	-0.96	-1.68	-0.78	-1.16	-0.22	-0.47
	Lateral Moment	-0.90	-0.20	0.50	0.25	-0.23	-0.32	0.37
C6 C5	Axial Moment	-0.27	-0.56	-0.20	-0.17	-0.23	0.00	-0.12
	Extension Moment	-1.60	-0.66	-1.45	-0.51	-0.85	0.18	-0.05
	Lateral Moment	-1.54	-0.45	0.68	0.41	0.41	-0.57	0.60
C7 C6	Axial Moment	-0.05	-0.09	-0.25	-0.23	-0.18	0.10	-0.24
	Extension Moment	-0.50	0.32	-0.31	0.41	0.31	1.27	1.19
	Lateral Moment	-2.16	-0.72	0.86	0.60	-0.49	-0.83	0.85
Sacrum Pelvis	Axial Moment	-0.01	-0.02	0.01	0.02	0.01	-0.02	0.04
	Flexion Extension Moment	1.32	0.49	0.81	0.49	0.88	0.44	1.85
	Lateral Moment	0.02	0.03	-0.01	-0.03	-0.01	0.03	-0.06
T1 C7	Axial Moment	0.16	-0.01	-0.31	-0.27	-0.15	0.18	-0.38
	Extension Moment	0.84	1.42	1.09	1.40	1.66	2.42	2.58
	Lateral Moment	-2.83	-2.83	1.06	0.85	-0.61	-1.15	1.17

cord injury (SCI) during the seven phases of the gait cycle (Phases 1-7).

The simulations examined spinal loading with exoskeleton assistance in individuals with complete spinal cord injury (SCI). Lower-limb muscles were deactivated to represent the assumed loss of motor function. The exoskeleton was incorporated into the musculoskeletal model, and loads were estimated in the cervical, sacrum–pelvis, and thoracic regions.

In the cervical spine, the extension moment decreased by 46%, overall joint loading by 30%, and the lateral bending moment by 88%. At the sacrum–pelvis joint, the corresponding reductions were 91%, 85%, and 92%.

The thoracic region showed a 97% reduction in the extension moment and a 71% reduction in the lateral bending moment. Overall joint loading decreased by 8%, a smaller change than those observed in the two moment components.

Exoskeleton assistance reduced these loading measures in all three regions under the specified model conditions. However, the simulations did not assess pain, stability, fatigue, or long-term tissue changes. Experimental measurements and clinical assessments are needed before these estimates can inform rehabilitation decisions.

Exoskeletons provide external support during movement and may alter loads within the musculoskeletal system. In people with spinal cord injury (SCI), this support can assist walking when lower-limb motor function is impaired. However, the effects on individual spinal joints depend on the device, task, and user. This study used the AnyBody Modeling System to compare estimated spinal forces and moments during walking in healthy participants and participants with SCI.

Previous studies have examined exoskeleton assistance during lifting and other physically demanding tasks. Passive back-support devices have been reported to reduce trunk extensor muscle activity by 10–28% and energy expenditure by 4–13% [28, 29]. These findings concern different tasks and device types, so they cannot be directly transferred to lower-limb exoskeleton-assisted walking. Studies have also evaluated AnyBody predictions against experimental measurements [30]. Such validation does not establish the accuracy of every model configuration, including the one used here.

Task-specific evaluations are needed because loading patterns may change with walking speed, slope, carried loads, and exoskeleton design [31]. The present study combined recorded joint kinematics with musculoskeletal modeling to examine spinal loading under selected walking conditions. Healthy walking was modeled with and without an exoskeleton. For participants with SCI, assisted walking was compared with a theoretical unassisted condition. This theoretical condition was a computational reference, rather than an observed walking trial.

The reported average reduction in spinal joint forces was 25–30% during exoskeleton-assisted gait. Cervical forces decreased by up to 40%, while lumbar forces decreased by approximately 30%. These estimates indicate lower loading for the reported comparisons. They should be interpreted alongside the joint-specific and directional results, which included both reductions and increases in some moment components. Exoskeleton assistance therefore did not produce a uniform change across the spine.

The reductions are consistent with reports of load redistribution during exoskeleton use [32]. However, differences in device design, model assumptions, and movement conditions limit direct comparisons between studies. Lower cervical forces do not, by themselves, establish improved upper-body stability or reduced neck strain. Likewise, lower lumbar forces do not demonstrate pain relief or protection against injury. Previous reports on cervical and lumbar unloading provide context for these findings [28, 33], but clinical outcomes require separate assessment.

The exoskeleton frame was made from A-grade fiberglass. Lightweight materials have also been considered in other exoskeleton designs [34]. This study did not compare different frame materials, so the loading reductions cannot be attributed specifically to fiberglass. Its effects on device mass, structural behavior, and mobility would need to be evaluated through material and device testing.

Several limitations affect the interpretation of the results. The study included four participants from the Adana region of Türkiye: two healthy individuals and two individuals with SCI. Height and body mass were matched within the male and female pairs. This reduced variation in those characteristics, but it did not account for other differences between participants. The sample was too small to estimate population-level effects or examine variation in injury characteristics.

The recordings were obtained under laboratory conditions. Participants with SCI used a Robogait rehabilitation system, while healthy participants walked on a treadmill. Differences between these arrangements may have influenced the recorded movements and subsequent load estimates. Only two gait cycles were recorded for each participant with SCI. These recordings provide limited information about variation between cycles or changes during longer walking sessions.

The SCI simulations assumed inactive lower-limb muscles. The model also treated body segments as rigid and did not represent soft tissue deformation. These assumptions simplify the modeled interaction between the person and the exoskeleton. The estimated loads therefore depend on the specified muscle settings, joint constraints, attachment points, and movement inputs. No independent validation of the spinal load estimates was reported for this study.

Further work should include more participants with a wider range of injury levels, body dimensions, and walking abilities. Repeated trials could help assess the consistency of the estimates. Analyses at different speeds, on slopes, and

under additional loading conditions would clarify how task demands affect spinal loading. Device fit, attachment position, and mass distribution should also be examined.

Longer-term studies are needed to assess comfort, fatigue, pain, and rehabilitation outcomes. Comparisons with experimental measurements would help evaluate the model predictions. Until such evidence is available, the present findings should be treated as case-level simulation results describing how exoskeleton assistance changed estimated spinal loads under the selected conditions.

CONCLUSION

This study used the AnyBody Modeling System to estimate spinal loads during walking in healthy individuals and people with complete spinal cord injury (SCI). In the reported comparisons, cervical joint forces decreased by approximately 40% and lumbar joint forces by 30% with exoskeleton assistance. The changes were not uniform. Some joint moments increased even when other loading measures decreased.

Recorded joint movements were used to compare forces and moments across gait phases. The study included four participants, and unassisted walking in the SCI models was a theoretical reference rather than an observed trial. The results therefore apply to these cases and the assumptions used in the simulations.

The exoskeleton had an A-grade fiberglass frame. No other materials were tested, so the study could not isolate the effect of fiberglass on loading or device performance. Pain, postural stability, injury prevention, and rehabilitation outcomes were also not assessed. Workplace applications would need to be evaluated separately.

Further studies should include more participants and repeated walking trials at different speeds, on slopes, and with carried loads. They should also examine device alignment, attachment position, and individual anatomy. Experimental measurements are needed to check the estimated loads. Longer-term clinical studies could then assess whether these changes benefit users.

AUTHORSHIP CONTRIBUTIONS

İsmail Çalıkuşu and Uğur Fidan contributed equally to this study. İsmail Çalıkuşu was responsible for data collection, processing, and initial analysis, as well as contributing to the writing and structuring of the manuscript. Uğur Fidan was involved in data analysis, interpretation, and refinement of the manuscript, ensuring the integration of findings into the broader biomechanical and exoskeleton research context. Both authors collaboratively participated in the conceptualization, methodological design, and final revision of the study, ensuring its academic rigor and coherence.

DATA AVAILABILITY STATEMENT

The authors confirm that the data that supports the findings of this study are available within the article. Raw data that support the finding of this study are available from the corresponding author, upon reasonable request.

CONFLICT OF INTEREST

The authors declared that there is no conflict of interest associated with this study.

ETHICS

There are no ethical issues with the publication of this manuscript.

STATEMENT ON THE USE OF ARTIFICIAL INTELLIGENCE

Artificial intelligence was not used in the preparation of the article.

REFERENCES

[1] Dunkelberger N, Schearer EM, O'Malley MK. A review of methods for achieving upper limb movement following spinal cord injury through hybrid muscle stimulation and robotic assistance. Exp Neurol 2020;328:113274. [CrossRef]

[2] Powell MP, Verma N, Sorensen E, Carranza E, Boos A, Fields DP, et al. Epidural stimulation of the cervical spinal cord for post-stroke upper-limb paresis. Nat Med 2023;29:689–699. [CrossRef]

[3] Plaza A, Hernandez M, Puyuelo G, Garces E, Garcia E. Lower-limb medical and rehabilitation exoskeletons: a review of the current designs. IEEE Rev Biomed Eng 2023;16:278–291. [CrossRef]

[4] Steinhilber B, Seibt R, Rieger MA, Luger T. Postural control when using an industrial lower limb exoskeleton: impact of reaching for a working tool and external perturbation. Hum Factors 2022;64:635–648. [CrossRef]

[5] Meenakshi S, Balasankar SK. Analysis of work-flow design related to aspects of productivity and ergonomics. In: International Conference on Human-Computer Interaction; 2023. Springer. [CrossRef]

[6] Engelhardt L, Melzner M, Havelkova L, Fiala P, Christen P, Dendorfer S, et al. A new musculoskeletal AnyBody™ detailed hand model. Comput Methods Biomech Biomed Engin 2020;24:777–787. [CrossRef]

[7] Cao L, Zhang J, Zhang P, Fang D. Research on the influence of exoskeletons on human characteristics by modeling and simulation using the AnyBody Modeling System. Appl Sci 2023;13:8184. [CrossRef]

[8] Gullison AJ. The interaction between over-ground exoskeleton gait training and muscle spasticity. 2021.
[9] Asadı Dereshgı H, Serbest K, Şahin SN, Balık B. Skeletal muscle mechanics from Hill-based muscle model to computer applications: state of the art review. J Smart Syst Res 2021;2:27–39.
[10] Behjati Ashtiani M, Akhavanfar M, Li L, Kim S, Nussbaum MA. Using musculoskeletal models to estimate the effects of exoskeletons on spine loads during dynamic lifting tasks: differences between OpenSim and the AnyBody modelling system. J Biomech 2025;188:112780. [CrossRef]
[11] Alexander N, Schwameder H, Baker R, Trinler U. Effect of different walking speeds on joint and muscle force estimation using AnyBody and OpenSim. Gait Posture 2021;90:197–203. [CrossRef]
[12] Caimi A, Ferguson SJ, Ignasiak D. Evaluation of trunk muscle coactivation predictions in multibody models. J Biomech 2024;168:112039. [CrossRef]
[13] Mak SKD, Accoto D. Review of current spinal robotic orthoses. Healthcare (Basel) 2021. [CrossRef]
[14] Kern M, Velasquez-Ignacio C, Afzal T, Tseng SC, Francisco GE, Chang SH. Priming with transcutaneous spinal direct current stimulation followed by robotic exoskeleton gait training in individuals with spinal cord injury: a case series. J Spinal Cord Med 2025;48:1146–1153. [CrossRef]
[15] Liu P, Cheng Y, Xu Z, Li X, Chen Z, Duan W. Spatiotemporal spinal cord stimulation with real-time triggering exoskeleton restores walking capability: a case report. Ann Clin Transl Neurol 2025;12:659–665. [CrossRef]
[16] Liu P, Cheng Y, Xu Z, Li X, Chen Z, Duan W. Spatiotemporal spinal cord stimulation with real-time triggering exoskeleton restores walking capability: a case report. Ann Clin Transl Neurol 2025;12:659–665. [CrossRef]
[17] Chen Y, Yin W, Zheng L, Mehta R, Zhang X. Biodynamic modeling and analysis of human-exoskeleton interactions in simulated patient handling tasks. Hum Factors 2025;67:641–655. [CrossRef]
[18] Chandran VD, Nam S, Hexner D, Bauman WA, Pal S. Comparison of the dynamics of exoskeletal-assisted and unassisted locomotion in an FDA-approved lower extremity device: controlled experiments and development of a subject-specific virtual simulator. PLoS One 2023;18:e0270078. [CrossRef]
[19] Arefeen A, Xia T, Xiang Y. Human-exoskeleton coupling simulation for lifting tasks with shoulder, spine, and knee-joint powered exoskeletons. Biomimetics (Basel) 2024;9:454. [CrossRef]
[20] Fritzsche L, Galibarov PE, Gärtner C, Bornmann J, Damsgaard M, Wall R, et al. Assessing the efficiency of exoskeletons in physical strain reduction by biomechanical simulation with AnyBody Modeling System. Wearable Technol 2021;2:e6. [CrossRef]
[21] Małek M, Jackowski M, Łasica W, Kadela M, Wachowski M. Mechanical and material properties of mortar reinforced with glass fiber: an experimental study. Materials (Basel) 2021;14:698. [CrossRef]
[22] Beng K, Aydil S, Özkan P. Üç boyutlu bilgisayarlı yürüme analizi: kinematik ve kinetik. TOTBİD Derg 2014;13:337–343. [CrossRef]
[23] Kapula PR, Reddy BV, Sushannth B, Srikar BS, Deekonda A, Jyothsna C. Creating models for 3D printing using Kinect based scanners. In: 2022 7th International Conference on Communication and Electronics Systems (ICCES); 2022. p. 261–265. [CrossRef]
[24] Çalıkuşu İ, Uzunhisarcıklı E, Fidan U. Alt ekstremite dış iskeletinin modellenmesi ve biyomekanik analizi. Gazi Univ Muhendis Mimarlik Fak Derg 2024;39:549–562. [CrossRef]
[25] Akhavanfar M, Mir-Orefice A, Uchida TK, Graham RB. An enhanced spine model validated for simulating dynamic lifting tasks in OpenSim. Ann Biomed Eng 2024;52:259–269. [CrossRef]
[26] Rasmussen J. The AnyBody modeling system. In: DHM and Posturography; 2019. p. 85–96. [CrossRef]
[27] North K, Jones ST, Simpson GM, Dalrymple AN. Personalized gait rehabilitation with spinal cord stimulation and machine learning: recent advances and promising applications. Curr Opin Biomed Eng 2025;34:100579. [CrossRef]
[28] Madinei S, Nussbaum MA. Estimating lumbar spine loading when using back-support exoskeletons in lifting tasks. J Biomech 2023;147:111439. [CrossRef]
[29] Eskandari AH, Ghezelbash F, Shirazi-Adl A, Arjmand N, Larivière C. Effect of a back-support exoskeleton on internal forces and lumbar spine stability during low load lifting task. Appl Ergon 2025;123:104407. [CrossRef]
[30] Auer S, Tröster M, Schiebl J, Iversen K, Chander DS, Damsgaard M, et al. Biomechanical assessment of the design and efficiency of occupational exoskeletons with the AnyBody Modeling System. Z Arbeitswiss 2022;76:440–449. [CrossRef]
[31] Abery P, Canetti EFD, Hing W. The role of lower limb exoskeletons in rehabilitation: a scoping review. Phys Ther Rev 2025;30:118–136. [CrossRef]
[32] Sahu N, Ganesan K, Gupta A. Simulation-based analysis and design of passive back exoskeleton for squat lifting. J Eng Sci Med Diagn Ther 2025;8. [CrossRef]
[33] Firouzi V, Seyfarth A, Song S, von Stryk O, Sharbafi MA. Biomechanical models in the lower-limb exoskeletons development: a review. J Neuroeng Rehabil 2025;22:12. [CrossRef]
[34] Zhou Y. User experience of lower extremity exoskeletons and its improvement methodologies: a narrative review. Proc Inst Mech Eng H 2024;238:1052–1068. [CrossRef]